

Performance of Rake Reception in Dense Multipath Channels: Implications of Spreading Bandwidth and Selection Diversity Order

Moe Z. Win, *Senior Member, IEEE*, George Chrisikos, *Member, IEEE*, and Nelson R. Sollenberger, *Fellow, IEEE*

Abstract—In this paper, we develop an analytical framework to quantify the effects of the spreading bandwidth (BW) on spread spectrum systems operating in dense multipath environments in terms of the receiver performance, the receiver complexity, and the multipath channel parameters. The focus of the paper is to characterize the symbol error probability (SEP) performance of a Rake receiver tracking the L strongest multipath components in wide-sense stationary uncorrelated scattering (WSSUS) Gaussian channels with frequency-selective fading. Analytical SEP expressions of the Rake receiver are derived in terms of the number of combined paths, the spreading BW, and the multipath spread of the channel. The proposed problem is made analytically tractable by transforming the physical Rake paths, which are correlated and ordered, into the domain of a “virtual Rake” receiver with independent virtual paths. This results in a simple derivation of the SEP for a given spreading BW and an arbitrary number of combined paths.

Index Terms—Dispersive channels, diversity methods, fading channels, maximal ratio combining, Rake receiver, selection diversity, spreading bandwidth, spread spectrum techniques, virtual path technique.

I. INTRODUCTION

MULTIPLE access systems, based on spread spectrum (SS) signaling properties, are suitable for dealing with fading multipath channels [1], [2]. These SS multiple access techniques have recently seen significant deployment in wireless communications systems, and they have also been proposed for third-generation wireless access [3]. One benefit of SS systems is that with a sufficiently wide transmission bandwidth (BW), it is possible to resolve the closely spaced multipath components encountered in the channel. Alternatively, systems using narrowband transmissions perceive most of the closely spaced multipath components as a single faded signal.

The detection of signals in a multipath environment leads to a Rake receiver, which is based on optimality theory tempered by some heuristic ideas. Rake receivers resolve the components of a received signal (arriving at different times) and combine them to provide diversity. Discussions on classical Rake receivers can

be found in [4]–[7]. One version of the Rake receiver consists of multiple correlators (fingers) where each of the fingers can detect/extract the signal from one of the multipath components created by the channel. The outputs of the fingers are combined to reap the benefits of Rake diversity.

The equivalent matched filter version of the receiver involves a matched front-end processor (MFEP) (matched *only* to the transmitted signature waveform) followed by a tapped delay line and a combiner. Multipath components with delays greater than the chip time T_c (approximately equal to the inverse of the spreading BW) apart are resolved by the MFEP, which is synchronized with the initial path of the received signal. The MFEP output is passed through a tapped delay line filter with $N_r = T_d/T_c$ taps, where T_d is the maximum excess delay from the first arriving path. The output of the taps provide N_r diversity paths, all of which must be combined for the best possible performance.

We introduce the term *all Rake (ARake)* receiver to describe the receiver with unlimited resources (taps or correlators) and instant adaptability, so that it can, in principle, combine *all* of the resolved multipath components. For a dense multipath channel with a fixed T_d , the number of resolvable multipath components N_r increases with the spreading BW. However, the number of multipath components that can be utilized in a typical Rake combiner is limited by power consumption issues, design complexity, and the channel estimation [8].

Complexity and performance issues have motivated studies of multipath combining receivers that process only a *subset* of the available N_r resolved multipath components, but achieve better performance than a single path (SP) receiver. We will refer to such receivers as *selective Rake (SRake)* receivers. This paper considers the SRake receiver that selects the L best paths with the largest signal-to-noise ratio (SNR) (from N_r available diversity paths) and combines them using maximal-ratio combining (MRC) [7].

For a given transmission BW and for a typical power delay profile (PDP), a fundamental question related to the SRake receiver design is the impact of the number of combined paths on the symbol error probability (SEP) performance, and what is the performance improvement versus complexity tradeoff. From the receiver complexity point of view, the question can be rephrased: For a fixed complexity receiver operating in an environment with a given PDP, what is the optimal spreading BW to be used.

Manuscript received August 1999; revised February 28, 2000. This paper was presented in part at the IEEE Wireless Communications and Networking Conference, New Orleans, LA USA, September 1999.

M. Z. Win and N. R. Sollenberger are with the Wireless Systems Research Department, Newman Springs Laboratory, AT&T Labs–Research, Red Bank, NJ 07701-7033 USA (e-mail: win@research.att.com; nelson@research.att.com).

G. Chrisikos is with Dot Wireless, Inc., San Diego, CA 92121 USA (e-mail: chrisiko@milly.usc.edu).

Publisher Item Identifier S 0733-8716(00)06118-7.

The design of receivers for code division multiple access (CDMA) systems, and in particular the choice of the number of combined paths, is often based on simulations and empirical knowledge [3], [9], [10]. Recently, some theoretical and simulation-based efforts have been made to investigate the effects of multipath fading [11]–[13]. Typical studies on the performance of direct sequence code division multiply access (DS-CDMA) as a function of the number of Rake fingers assume an ARake model ($L = N_r$) [14], [15]. In [16] and [17], the channel is modeled to consist of several groups of paths, where one dominant path per group is combined in the receiver.

However, as pointed out in [15], a more realistic model is the Rake receiver tracking the L strongest out of N_r paths. In fact, quasianalytical/experimental analysis of the ultra-wide BW SRake receiver (with large N_r) in [18] shows that an acceptable level of SEP performance can be achieved even with $L = 1$ and $L = 2$. This indicates that a high diversity order can be achieved even with a selection diversity (SD) or SP receiver. If one were to use an ARake model to analyze such a system, the results would be misleading in that it would suggest requiring more fingers. In [19], only $L = 2$ and $L = 3$ out of N_r paths were analyzed. The dependence of the signal power variance on the receiver processing in terms of parameters such as chip rate, processing gain, and number of multipath components tracked is investigated for $L = 1, 2, 4,$ and 8 through simulations in [13]. The bit error rate performance of an SRake receiver was analyzed in [20] for binary differential phase shift-keying modulation.¹ A closely related problem of hybrid selection/maximal-ratio combining (H-S/MRC) receivers in a more general diversity setting was considered in [21] and [22].

The principal contributions of this paper are in discovering a methodology and deriving exact SEP expressions of the SRake receiver for arbitrary L and N_r (i.e., arbitrary spreading BW). We develop an analytical framework to quantify the effects of spreading BW on SS systems operating in dense multipath environments in terms of the receiver complexity and multipath channel parameters. We assume that instantaneous estimation of all possible multipaths is feasible, such as with slow fading. However, SRake combining also offers improvement in fast fading conditions, and our results serve as a bound on the performance when ideal channel estimates are not available. The proposed problem is made analytically tractable by transforming the physical Rake paths into the domain of a “virtual Rake” receiver, which results in a simple derivation of the SEP for a given spreading BW and an *arbitrary* number of combined paths.

We first derive general expressions, and then focus on the special case of constant PDP over an interval. Several researchers have previously considered this type of PDP [23]–[25], [15] to study various aspects of DS-CDMA systems. Propagation mea-

surements in urban and suburban environments [26]–[28] and mountainous terrain [29] exhibit characteristics supporting such a PDP since they show channels with energy spread over a continuum of arrival times. Thus, the use of this PDP serves as a basic model for analyzing the performance of Rake receivers operating in dense multipath environments. We plot the SEP results obtained and observe the property of diminishing returns with an increase in the number of combined paths. The well-known results for the SP receiver and the ARake receiver can be obtained as special cases of the SRake receiver results.

Second-generation cellular systems which are based on CDMA (IS-95) operate at a chip rate of 1.2288 Mchips/s, and the third-generation (e.g., IMT-2000) systems will most probably operate at 3.84 Mchips/s. To support higher bit rates, larger spreading BW’s have been proposed [3]. As the third-generation activities progress, the designers of receivers will face the question of how many fingers should be included in Rake receivers, and/or how many fingers should be active at any one time. The results of this paper provide part of the necessary inputs for making those decisions.

II. SYSTEM MODEL

A. Signal and Channel Models

The output of the channel is modeled as²

$$\tilde{y}(t) = \Re \{ y(t) e^{j2\pi f_c t} \} \quad (1)$$

where $y(t)$ is the equivalent lowpass (ELP) output signal. The ELP channel output $y(t)$ can be expressed in terms of the ELP transmitted signal $s(t)$, with energy $2E_s$, in the time domain as

$$y(t) = \int_{-\infty}^{+\infty} h(t, \tau) s(t - \tau) d\tau \quad (2)$$

where $h(t, \tau)$ is the ELP time-variant channel impulse response, with t and τ denoting the time and delay variables, respectively. For a physical channel, $h(t, \tau)$ must have finite support over the positive values of τ , satisfying the causality condition. The function $h(t, \tau)$ is typically referred to as the input-delay spread function representing the response of the channel at time t due to an impulse applied at time $t - \tau$ [30], [31].

The ELP received signal can be modeled as

$$r(t) = y(t) + n(t) \quad (3)$$

where $n(t)$ is an additive white Gaussian noise (AWGN) process with two-sided power spectral density $2N_0$.³ The additive noise process $n(t)$ is independent of the channel $h(t, \tau)$ and therefore independent of the process $y(t)$ [see (2)].

B. Matched Front-End Processor

Consider a matched front-end processor (MFEP) with ELP impulse response

$$f_M(t) = \begin{cases} s^*(T_s - t), & 0 < t < T_s \\ 0, & \text{otherwise} \end{cases} \quad (4)$$

²The notation $\Re\{\cdot\}$ denotes the real-part operator.

³The term “Gaussian” is used to denote “ELP complex circular Gaussian.”

¹In [20], the probability density function (p.d.f.) of the sum of the signals with the L strongest path SNR’s was obtained as a convolution of the p.d.f.’s of the strongest, the second strongest, . . . , and the L^{th} strongest paths. We remark that, in general, the p.d.f. of the sum of the random variables is the convolution of the individual p.d.f.’s only if the random variables are independent.

where T_s is the symbol duration. The MFEP output can be written as⁴

$$r_M(t) = \int_0^{+\infty} r(t - \alpha) f_M(\alpha) d\alpha. \quad (5)$$

Substituting (3) into (5), the MFEP output can be written as

$$r_M(t) = y_M(t) + n_M(t) \quad (6)$$

where $y_M(t)$ and $n_M(t)$ are the contributions of the signal and noise, respectively, to the MFEP output.

Using (2), the process $y_M(t)$ can be written as

$$y_M(t) = \int_0^{+\infty} \int_{-\infty}^{+\infty} h(t - \alpha, \tau) s(t - \alpha - \tau) f_M(\alpha) d\tau d\alpha. \quad (7)$$

The noise process $n_M(t)$ is given by

$$n_M(t) = \int_0^{+\infty} n(t - \alpha) f_M(\alpha) d\alpha. \quad (8)$$

III. SRAKE RECEIVER PERFORMANCE ANALYSIS

In this section, the theory developed in [22] for a more general diversity setting is applied to the study of an SRake receiver with an arbitrary number of combined paths in a frequency-selective dense multipath channel.

A. The SRake Receiver

Let γ_i denote the instantaneous SNR of the MFEP output samples defined by

$$\gamma_i \triangleq \frac{|y_M(t_i)|^2}{\mathbb{E}\{|n_M(t_i)|^2\}} \quad (9)$$

where t_i 's are the sampling instants. We model the γ_i 's as continuous random variables with p.d.f. $f_{\gamma_i}(x)$ and mean

$$\Gamma_i = \mathbb{E}\{\gamma_i\} = \frac{\mathbb{E}\{|y_M(t_i)|^2\}}{\mathbb{E}\{|n_M(t_i)|^2\}}. \quad (10)$$

The instantaneous output SNR of the SRake receiver is

$$\gamma_{\text{SRake}} = \sum_{i=1}^L \gamma_{(i)} \quad 1 \leq L \leq N_r \quad (11)$$

where $\gamma_{(i)}$ is the ordered γ_i , i.e., $\gamma_{(1)} > \gamma_{(2)} > \dots > \gamma_{(N_r)}$, and N_r is the number of resolvable multipath components. As pointed out in the prequel, N_r increases with the spreading BW. It is apparent that several multipath combining receivers such as the SP and ARake receivers turn out to be special cases of (11).

We model the time-varying channel $h(t, \tau)$ as a two-dimensional complex circular Gaussian process with zero mean. Since $y_M(t)$ is a linear transformation of $h(t, \tau)$ [cf. (7)], it is also a complex Gaussian process with zero mean and correlation function $R_y(t_1, t_2)$. For a wide-sense stationary uncorrelated scattering (WSSUS) channel with constant PDP, it can be shown

⁴Since the rest of the paper deals with the ELP notation, we shall drop the term ELP in the sequel. Here, and throughout the paper, the range of the integration is determined by the support of the integrand.

using (43) of the Appendix that the correlation function of the MFEP output samples is⁵

$$R_y(t_1, t_2) = \begin{cases} 4\beta \frac{T_c}{T_d} E_s^2, & |t_2 - t_1| = 0 \\ 4\tilde{\beta} \frac{T_c}{T_d} E_s^2, & |t_2 - t_1| = T_c \\ 0, & |t_2 - t_1| = kT_c \quad k = 2, 3, \dots \end{cases} \quad (12)$$

The coefficients β and $\tilde{\beta}$ depend on the specific chip pulse shape. We consider three types of pulse shapes in this paper, namely the rectangular, half-sine, and raised cosine pulse shapes. Each pulse shape has finite support over the interval $[0, T_c)$ and is normalized to constant energy. Such time limited pulse shapes have been used previously in the literature [32]. The rectangular pulse shape is defined by $p_{T_c}(t) = 1$, $0 \leq t < T_c$. Similarly, the expressions for the half-sine and raised cosine pulse shapes are given by $\sqrt{2} \sin(\pi t/T_c) p_{T_c}(t)$ and $\sqrt{2/3} [1 - \cos(2\pi t/T_c)] p_{T_c}(t)$, respectively. The coefficients β and $\tilde{\beta}$ are straightforward to compute and are given by the following expressions:

$$\beta = \begin{cases} \frac{2}{3}, & \text{rectangular pulse} \\ \frac{5}{2\pi^2} + \frac{1}{3}, & \text{half-sine pulse} \\ \frac{35}{24\pi^2} + \frac{1}{3}, & \text{raised cosine pulse} \end{cases} \quad (13)$$

and

$$\tilde{\beta} = \begin{cases} \frac{1}{6}, & \text{rectangular pulse} \\ \frac{5}{4\pi^2} - \frac{1}{12}, & \text{half-sine pulse} \\ \frac{1}{12} - \frac{35}{48\pi^2}, & \text{raised cosine pulse.} \end{cases} \quad (14)$$

Numerically, $\beta = 0.6666, 0.5866, 0.4811$ and $\tilde{\beta} = 0.1666, 4.332 \times 10^{-2}, 9.453 \times 10^{-3}$ for the rectangular, half-sine, and raised cosine pulses, respectively.

The correlation function $R_y(t_1, t_2)$ given in (12) implies that samples of the MFEP output are uncorrelated as long as they are not adjacent to each other. It also implies that even the adjacent samples are "weakly correlated" with correlation coefficient equal to 0.25, 0.07386, and 0.01965 for the rectangular, half-sine, and raised cosine pulse shapes, respectively. Motivated further by analytical tractability, the MFEP output samples are modeled to be uncorrelated. Therefore, they are independent since $y_M(t)$ is a complex Gaussian process.⁶

Denoting $\boldsymbol{\gamma}_{(N_r)} \triangleq (\gamma_{(1)}, \gamma_{(2)}, \dots, \gamma_{(N_r)})$, it was shown in [22] that the joint p.d.f. of $\gamma_{(1)}, \gamma_{(2)}, \dots, \gamma_{(N_r)}$ is, see (15) at the bottom of the next page. The parameter Γ is the mean SNR of the MFEP output given by

$$\Gamma = \frac{R_y(t_1, t_1)}{R_n(t_1, t_1)} = \beta \frac{T_c}{T_d} \left(\frac{E_s}{N_0} \right) \quad (16)$$

⁵Although we are concerned only with the values of $|t_2 - t_1|$ at integer multiples of T_c in (12), $R_y(t_1, t_2)$ is in general a continuous function of $|t_2 - t_1|$ as can be seen in (43).

⁶This justifies the standard assumption of "independent MFEP output samples" made in typical studies concerning Rake receivers (e.g., [7], [14]).

where $R_n(t_1, t_2)$ is given by (45) of the Appendix. It is important to note that the $\gamma_{(i)}$'s are *no* longer independent, even though the underlying γ_i 's are independent.

B. Error Probability Analysis in Virtual Rake Framework

The SEP for an SRake receiver in a multipath fading environment can be written as

$$P_{e, \text{SRake}} = \mathbf{E}_{\gamma_{\text{SRake}}} \left\{ \Pr\{e | \gamma_{\text{SRake}}\} \right\} \quad (17)$$

where $\Pr\{e | \gamma_{\text{SRake}}\}$ is the *conditional* SEP, conditioned on the random quantity γ_{SRake} . For coherent detection of M -ary phase-shift keying (MPSK), an alternative representation for $\Pr\{e | \gamma_{\text{SRake}}\}$ involving a definite integral with *finite* limits, is given by [33] and [34] as

$$\Pr\{e_{\text{MPSK}} | \gamma_{\text{SRake}}\} = \frac{1}{\pi} \int_0^\Theta e^{-(\delta_{\text{MPSK}} / \sin^2 \theta) \gamma_{\text{SRake}}} d\theta \quad (18)$$

where $\delta_{\text{MPSK}} = \sin^2(\pi/M)$ and $\Theta = \pi(M-1)/M$. Of course, for BPSK, $\delta_{\text{MPSK}} = 1$ and $\Theta = \pi/2$. Substituting (18) into (17), the SEP of the SRake receiver becomes

$$P_{e, \text{SRake}} = \frac{1}{\pi} \int_0^\Theta \mathbf{E}_{\gamma_{\text{SRake}}} \left\{ e^{-(\delta_{\text{MPSK}} / \sin^2 \theta) \gamma_{\text{SRake}}} \right\} d\theta. \quad (19)$$

Substituting the expression for γ_{SRake} directly in terms of the physical branch variables given in (11) by using the technique of [35], we obtain

$$\begin{aligned} P_{e, \text{SRake}} &= \frac{1}{\pi} \int_0^\Theta \mathbf{E}_{\{\gamma_{(i)}\}} \left\{ \exp\left(-\frac{\delta_{\text{MPSK}}}{\sin^2 \theta} \sum_{i=1}^L \gamma_{(i)}\right) \right\} d\theta \quad (20) \\ &= \frac{1}{\pi} \int_0^\Theta \int_0^\infty \int_0^\infty \cdots \int_0^{\gamma_{(N_r-1)}} \exp\left(-\frac{\delta_{\text{MPSK}}}{\sin^2 \theta} \sum_{i=1}^L \gamma_{(i)}\right) \\ &\quad \times f_{\gamma_{(N_r)}}(\{\gamma_{(i)}\}_{i=1}^{N_r}) d\gamma_{(N_r)} \cdots d\gamma_{(2)} d\gamma_{(1)} d\theta. \quad (21) \end{aligned}$$

Since the statistics of the ordered paths are *no* longer independent, the evaluation of (21) involves N_r -fold nested integrals, which are in general cumbersome and complicated to evaluate. This can be alleviated by transforming the instantaneous SNR's of the ordered multipath components into a new set of *virtual path* instantaneous SNR's, V_n , using the following relationship:

$$\gamma_i = \sum_{n=i}^{N_r} \left[\beta \frac{T_c}{T_d} \left(\frac{E_s}{N_0} \right) \right] \frac{V_n}{n}. \quad (22)$$

Let $\mathbf{V}_{N_r} \triangleq [V_1, V_2, \dots, V_{N_r}]^t$, then the joint p.d.f. of V_1, V_2, \dots, V_{N_r} can be obtained as [36]

$$\begin{aligned} f_{\mathbf{V}_{N_r}}(\{V_n\}_{n=1}^{N_r}) &= J f_{\gamma_{(N_r)}}(\{\gamma_{(i)}\}_{i=1}^{N_r}) \Big|_{\gamma_{(i)} = \sum_{n=i}^{N_r} \left[\beta \frac{T_c}{T_d} \left(\frac{E_s}{N_0} \right) \right] (V_n/n)} \quad (23) \end{aligned}$$

where J is the Jacobian of the transformation.

First note that the recursion formula for the virtual path transformation is

$$\gamma_{(i)} = \gamma_{(i+1)} + \left[\beta \frac{T_c}{T_d} \left(\frac{E_s}{N_0} \right) \right] \frac{V_i}{i} \quad i = 1, \dots, N_r \quad (24)$$

where $\gamma_{N_r+1} = 0$. This implies that the virtual path transformation decouples the range of V_n 's, and $0 < V_n < \infty$. Since the transformation is linear, the Jacobian of the transformation can be calculated as

$$J = \frac{1}{N_r!} \left[\beta \frac{T_c}{T_d} \left(\frac{E_s}{N_0} \right) \right]^{N_r}. \quad (25)$$

Substituting (25) into (23), it can be verified after some algebra that the joint p.d.f. of V_1, V_2, \dots, V_{N_r} is

$$f_{\mathbf{V}_{N_r}}(\{V_n\}_{n=1}^{N_r}) = \begin{cases} \exp\left(-\sum_{n=1}^{N_r} V_n\right), & 0 \leq V_n < \infty \\ 0, & \text{otherwise.} \end{cases} \quad (26)$$

Therefore, the instantaneous SNR's of the virtual paths are independent and identically distributed (i.i.d.) normalized exponential random variables with p.d.f. given by

$$f_{V_n}(v) = \begin{cases} e^{-v}, & 0 < v < \infty \\ 0, & \text{otherwise.} \end{cases} \quad (27)$$

The instantaneous SNR of the combiner output can now be expressed in terms of the instantaneous SNR's of the virtual paths as

$$\gamma_{\text{SRake}} = \sum_{n=1}^{N_r} b_n V_n \quad (28)$$

where the coefficients b_n are given by

$$b_n = \begin{cases} \left[\beta \frac{T_c}{T_d} \left(\frac{E_s}{N_0} \right) \right], & n \leq L \\ \left[\beta \frac{T_c}{T_d} \left(\frac{E_s}{N_0} \right) \right] \frac{L}{n}, & \text{otherwise.} \end{cases} \quad (29)$$

$$f_{\gamma_{(N_r)}}(\{\gamma_{(i)}\}_{i=1}^{N_r}) = \begin{cases} N_r! \left(\frac{1}{\Gamma} \right)^{N_r} \exp\left(-\frac{1}{\Gamma} \sum_{i=1}^{N_r} \gamma_{(i)}\right), & \gamma_{(1)} > \gamma_{(2)} > \cdots > \gamma_{(N_r)} > 0 \\ 0, & \text{otherwise} \end{cases} \quad (15)$$

Note that γ_{SRake} in (28) is now expressed in terms of i.i.d. virtual path variables as opposed to (11) where it was written in terms of dependent physical path variables.

Now the SEP for the SRake receiver can be reformulated in terms of i.i.d. virtual path variables by substituting (28) into (19) as

$$\begin{aligned} P_{e,\text{SRake}} &= \frac{1}{\pi} \int_0^\Theta \mathbb{E}_{\{V_n\}} \left\{ \exp \left(-\frac{\delta_{\text{MPSK}}}{\sin^2 \theta} \sum_{n=1}^{N_r} b_n V_n \right) \right\} d\theta \\ &= \frac{1}{\pi} \int_0^\Theta \int_0^\infty \int_0^\infty \dots \int_0^\infty \\ &\quad \times \exp \left(-\frac{\delta_{\text{MPSK}}}{\sin^2 \theta} \sum_{n=1}^{N_r} b_n v_n \right) \prod_{n=1}^{N_r} f_{V_n}(v_n) dv_n d\theta. \end{aligned} \quad (30)$$

Exploiting the fact that the V_n 's are independent, (30) becomes

$$\begin{aligned} P_{e,\text{SRake}} &= \frac{1}{\pi} \int_0^\Theta \prod_{n=1}^{N_r} \mathbb{E}_{V_n} \left\{ e^{-[\delta_{\text{MPSK}} b_n / \sin^2 \theta] V_n} \right\} d\theta \\ &= \frac{1}{\pi} \int_0^\Theta \prod_{n=1}^{N_r} \psi_{V_n} \left(-\frac{\delta_{\text{MPSK}} b_n}{\sin^2 \theta} \right) d\theta \end{aligned} \quad (31)$$

where $\psi_{V_n}(\cdot)$ is the characteristic function (c.f.) of V_n and is given by

$$\psi_{V_n}(j\nu) \triangleq \mathbb{E} \{ e^{+j\nu V_n} \} = \frac{1}{1 - j\nu}. \quad (32)$$

The effectiveness of the virtual path technique is apparent by observing that the expectation operation in (20) no longer requires an N_r -fold nested integration.

Substituting (32) into (31), the SEP for the SRake receiver becomes (33) shown at the bottom of the page. Thus, the derivation of the SEP for the SRake receiver involving the N_r -fold nested integrals in (21) essentially reduces to a single integral over θ involving trigonometric functions with finite limits. Note that the independence of the virtual path variables plays a key role in simplifying the derivations.

C. Special Case 1: The Single Path Receiver

The SP receiver, also known as the selection diversity receiver, is the simplest form of diversity system whereby the received signal is selected from *one* of N_r diversity paths. The output SNR of the SP receiver is

$$\gamma_{\text{SP}} = \max_i \{ \gamma_i \} = \gamma_{(1)}. \quad (34)$$

This is a special case of the SRake receiver with $L = 1$. Substituting $L = 1$ into (33), the SEP for the SP receiver becomes

$$P_{e,\text{SP}} = \frac{1}{\pi} \int_0^\Theta \prod_{n=1}^{N_r} \left[\frac{\sin^2 \theta}{\delta_{\text{MPSK}} \left[\beta \frac{T_c}{T_d} \left(\frac{E_s}{N_0} \right) \right] \frac{1}{n} + \sin^2 \theta} \right] d\theta. \quad (35)$$

D. Special Case 2: The ARake Receiver

For the ARake receiver, the signals from *all* Rake paths are weighted and combined to maximize the SNR at the combiner output. The output SNR of the ARake receiver is given by

$$\gamma_{\text{ARake}} = \sum_{i=1}^{N_r} \gamma_i = \sum_{i=1}^{N_r} \gamma_{(i)}. \quad (36)$$

Note again that the result for the ARake receiver can be obtained from the SRake results given in (33) by setting $L = N_r$, since ARake is a special case of SRake with $L = N_r$. Therefore, the SEP for the ARake receiver becomes

$$P_{e,\text{ARake}} = \frac{1}{\pi} \int_0^\Theta \left[\frac{\sin^2 \theta}{\delta_{\text{MPSK}} \left[\beta \frac{T_c}{T_d} \left(\frac{E_s}{N_0} \right) \right] + \sin^2 \theta} \right]^{N_r} d\theta. \quad (37)$$

IV. NUMERICAL EXAMPLES

In this section, the results derived in the previous section for the SRake receiver are illustrated using specific examples. Figs. 1–4 show the SEP versus the SNR, E_s/N_0 , for various spreading BW's or, equivalently, for various chip rates $R_c = 1/T_c$. We depict $R_c = 1, 5,$ and 10 MHz with maximum excess channel delay $T_d = 2 \mu\text{s}$ for BPSK modulation using rectangular chip pulse waveforms.⁷

In Figs. 1 and 2, the curves are parameterized by the number of paths L with the highest curve representing $L = 1$, or the single path (SP) receiver, in each graph. Each successively lower curve corresponds to an increasing L up to the maximum L denoted by N_r , or the ARake receiver performance. We see that an increase in the number of combined paths produces a lower SEP, but the improvement diminishes as the number of combined paths approaches N_r . For example, with 5 MHz spreading BW, Fig. 1 suggests that at an SEP of 10^{-4} , there is a 2.5 dB

⁷The SEP using other chip pulse waveforms, such as the half-sine and the raised cosine, is not significantly different from that obtained with the rectangular pulse shape. The difference is in the attenuation of the mean SNR, and for comparison purposes, the rectangular pulse suffices.

$$P_{e,\text{SRake}} = \frac{1}{\pi} \int_0^\Theta \left[\frac{\sin^2 \theta}{\delta_{\text{MPSK}} \left[\beta \frac{T_c}{T_d} \left(\frac{E_s}{N_0} \right) \right] + \sin^2 \theta} \right]^L \prod_{n=L+1}^{N_r} \left[\frac{\sin^2 \theta}{\delta_{\text{MPSK}} \left[\beta \frac{T_c}{T_d} \left(\frac{E_s}{N_0} \right) \right] \frac{L}{n} + \sin^2 \theta} \right] d\theta \quad (33)$$

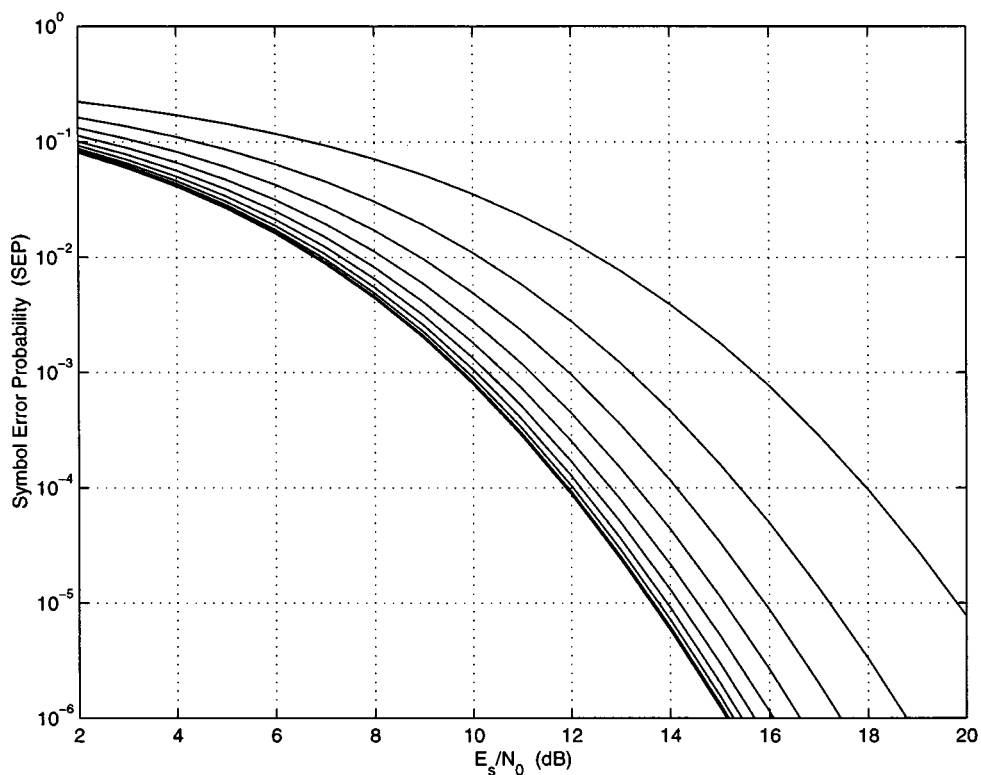


Fig. 1. The symbol error probability of the SRake receiver versus the SNR E_s/N_0 as a function of L for $R_c = 5$ MHz and $T_{\text{cl}} = 2 \mu\text{s}$. The upper curve is for $L = 1$ and the successively lower curves are for increasing L up to $L = N_r = 10$.

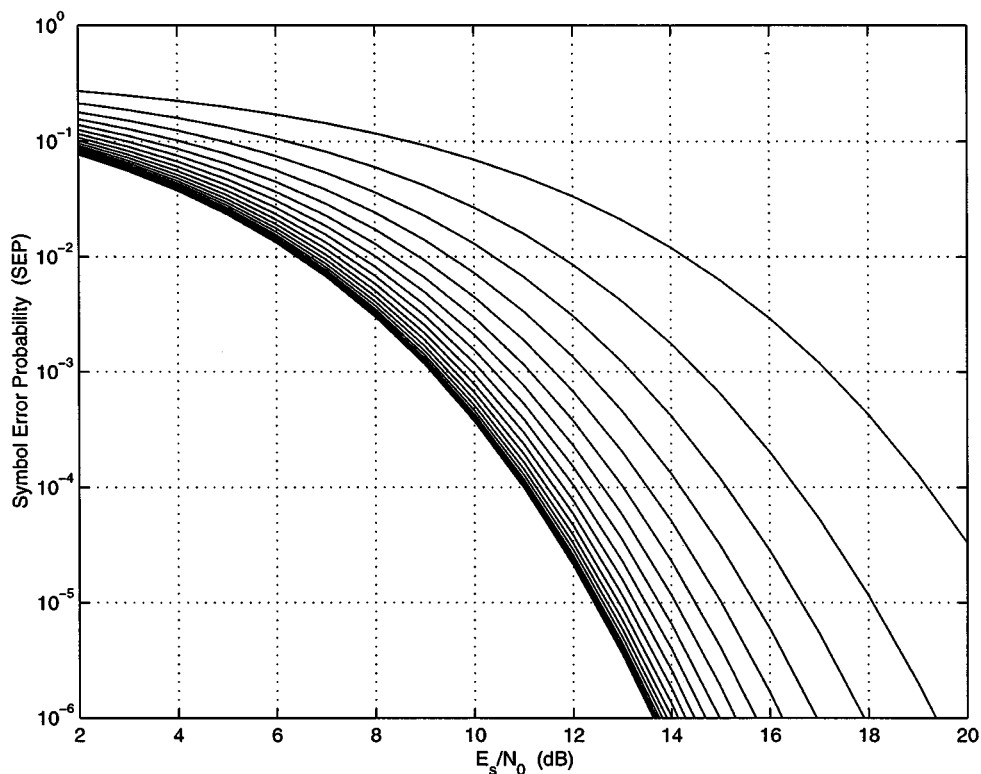


Fig. 2. The symbol error probability of the SRake receiver versus the SNR E_s/N_0 as a function of L for $R_c = 10$ MHz and $T_{\text{cl}} = 2 \mu\text{s}$. The upper curve is for $L = 1$ and the successively lower curves are for increasing L up to $L = N_r = 20$.

gain in using $L = 2$ paths from $L = 1$, but only over a 1 dB gain from $L = 2$ to 3. The gain in decibels diminishes further when L is increased from 3 to 4 and beyond. This trend is also

observed in Fig. 2 for the spreading BW of 10 MHz. The diminishing returns suggest that only a *subset* of paths need to be combined to give an acceptable level of performance.

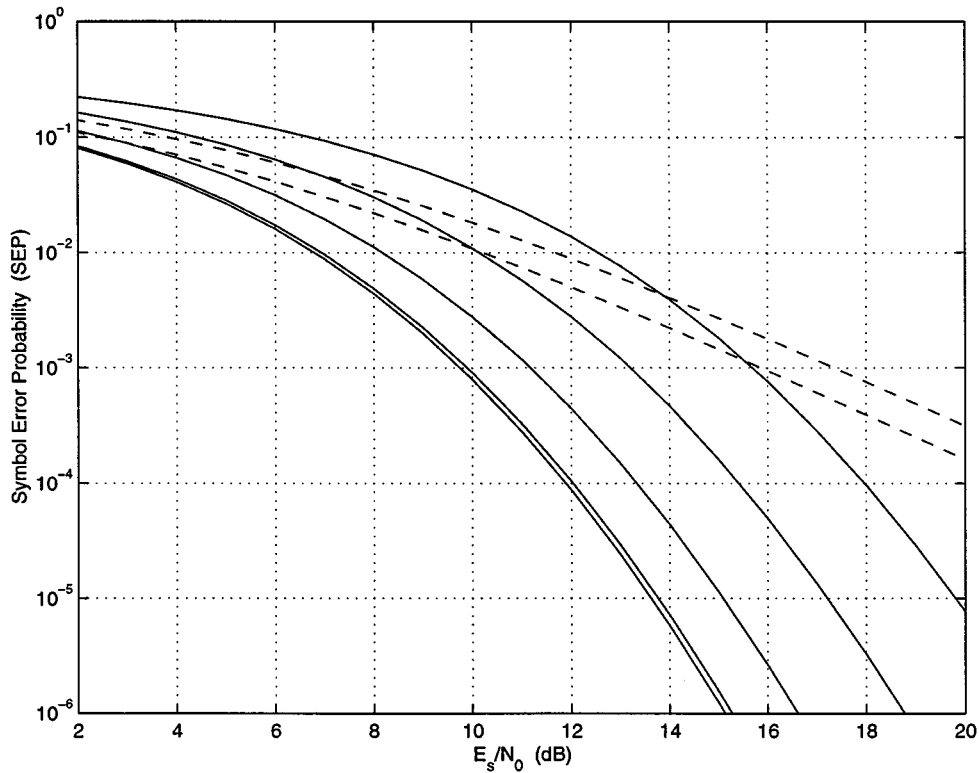


Fig. 3. The symbol error probability of the SRake receiver versus the SNR E_s/N_0 as a function of L with $T_d = 2 \mu\text{s}$. The dashed curves are for $R_c = 1 \text{ MHz}$ and the solid curves are for $R_c = 5 \text{ MHz}$. The solid curves depict $L = 1, 2, 4, 8,$ and 10 in successively lower positions. The dashed curves show $L = 1$ to $L = N_r = 2$.

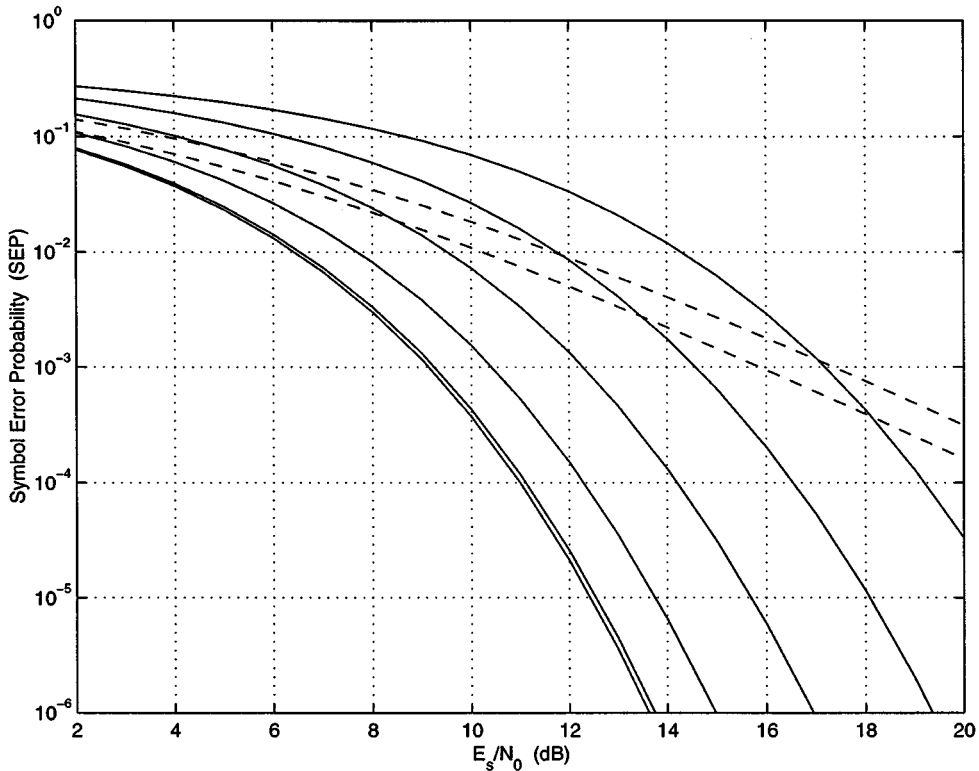


Fig. 4. The symbol error probability of the SRake receiver versus the SNR E_s/N_0 as a function of L with $T_d = 2 \mu\text{s}$. The dashed curves are for $R_c = 1 \text{ MHz}$ and the solid curves are for $R_c = 10 \text{ MHz}$. The solid curves depict $L = 1, 2, 4, 8, 16,$ and 20 in successively lower positions. The dashed curves show $L = 1$ to $L = N_r = 2$.

Figs. 3 and 4 compare the SEP of systems with $R_c = 1 \text{ MHz}$ and the case with $R_c = 5$ and 10 MHz . The dotted lines for $R_c = 1 \text{ MHz}$ are shown for $L = 1$ through 2 . The solid lines depict the larger BW signals with the number of paths L in-

creasing in powers of 2 up to N_r , i.e., $L = 1, 2, 4, 8, 16$, and 20 in Fig. 4. The effects of the diminishing returns and the wide range in SEP is evident as discussed above. It is also interesting to note the crossover in the curves between the two sets of R_c 's. For example, it can be seen in Fig. 4 that at SNR's above 8.5 dB, the SEP for $R_c = 10$ MHz with $L = 4$ is lower than the $R_c = 1$ MHz with $L = 2$ curve. But at SNR's below 8.5 dB, the $R_c = 10$ MHz with $L = 4$ curve gives a higher SEP than $R_c = 1$ MHz with $L = 2$. We see that at low SNR's, more paths need to be combined in the SRake receiver with larger BW's in order to achieve better performance than the SRake receiver with smaller BW's. For instance, L would have to be increased to about 8 in Fig. 4 for the $R_c = 10$ MHz case in order to achieve comparable performance with the $R_c = 1$ MHz with $L = 2$ case for low SNR's.

It is also observed that the larger the chip rate R_c , the lower the achievable SEP. With $R_c = 1$ MHz, the ARake receiver can only achieve an SEP of about 10^{-2} at an SNR of 10 dB. For $R_c = 5$ MHz, the ARake receiver can achieve an SEP of better than 10^{-3} at the same SNR. Alternatively, the ARake receiver with 10 MHz can achieve 4×10^{-4} SEP at about 10 dB, or a gain of 8 dB over the system with 1 MHz. The drawback in using a larger spreading BW is that a greater number of paths need to be combined to get better performance. If only one path is selected ($L = 1$), then the system with a smaller BW has a lower SEP over some range of SNR. This can be seen in Fig. 4 at 14 dB, for example.

It is apparent that a specified SEP can be achieved, in principle, with different combinations of receiver complexity (the number of combined paths L), spreading BW of the signals (R_c), and the transmitted power (SNR). For example, Fig. 3 shows that an SEP of 10^{-3} can be achieved with the combination of $R_c = 1$ MHz and $L = 2$, or with $R_c = 5$ MHz and $L = 8$. The performance difference between these cases is about 6 dB. Other combinations are also evident from the graphs. In general, larger spreading BW's reduce the power requirements as long as a sufficient number of paths are combined.

V. CONCLUSIONS AND COMMENTS

We derived exact SEP expressions for a selective Rake (SRake) receiver in a multipath fading environment. In particular, we considered frequency-selective wide-sense stationary uncorrelated scattering (WSSUS) Gaussian channels with constant power delay profile. We analyzed this system in the virtual Rake receiver domain which resulted in a simple derivation and formula of the SEP for a given spreading BW and an *arbitrary* number of combined paths. The key idea was to transform the dependent ordered-path variables into a new set of i.i.d. *virtual paths*, and express the combiner output SNR as a linear combination of the i.i.d. virtual path SNR variables. In this framework, the derivation of the SEP involving the evaluation of nested N -fold integrals, essentially reduces to the evaluation of a single integral.

For a fixed BW, the SEP decreases with an increase in the number of combined paths in the SRake receiver. The decrease in the achievable SEP is much greater for larger BW signals at the expense of the receiver complexity. As the number of

combined paths increases, the incremental gain in performance diminishes which suggest that only a *subset* of paths need to be combined to give an acceptable level of performance. In general, larger spreading BW's reduce the required power as long as a sufficient number of paths are combined. The results of this paper enable tradeoffs to be made between power, complexity, and BW to provide a specified SEP performance.

APPENDIX

STATISTICAL PROPERTIES OF THE MFEP OUTPUT

Statistical properties of $r_M(t)$ can be written in terms of the statistical properties of the random time-variant channel $h(t, \tau)$, and the additive noise $n(t)$. Using the fact that $n(t)$ is a zero-mean process, the mean value of the MFEP output process can be written as

$$\mathbf{E}\{r_M(t)\} = \int_0^{+\infty} \int_{-\infty}^{+\infty} \mathbf{E}\{h(t - \alpha, \tau)\} \times s(t - \alpha - \tau) f_M(\alpha) d\tau d\alpha. \quad (38)$$

Note that $r_M(t)$ is zero-mean if the two dimensional process $h(t, \tau)$ is zero-mean.

The correlation function of $r_M(t)$ is given by

$$R_r(t_1, t_2) = \mathbf{E}\{r_M^*(t_1)r_M(t_2)\}. \quad (39)$$

Since the noise $n(t)$ is zero mean and is independent of the time-variant channel $h(t, \tau)$, $R_r(t_1, t_2)$ becomes

$$R_r(t_1, t_2) = R_y(t_1, t_2) + R_n(t_1, t_2) \quad (40)$$

where $R_y(t_1, t_2)$ and $R_n(t_1, t_2)$ are correlation functions of $y_M(t)$ and $n_M(t)$, respectively.

It can be shown, using (7), that the correlation function of $y_M(t)$ is

$$R_y(t_1, t_2) = \int_0^{+\infty} \int_0^{+\infty} \int_{-\infty}^{+\infty} \int_{-\infty}^{+\infty} R_h(t_1 - \alpha_1, t_2 - \alpha_2; \tau_1, \tau_2) \times s^*(t_1 - \alpha_1 - \tau_1) f_M^*(\alpha_1) \times s(t_2 - \alpha_2 - \tau_2) f_M(\alpha_2) d\tau_1 d\tau_2 d\alpha_1 d\alpha_2 \quad (41)$$

where $R_h(t_1 - \alpha_1, t_2 - \alpha_2; \tau_1, \tau_2)$ is defined to be

$$R_h(t_1 - \alpha_1, t_2 - \alpha_2; \tau_1, \tau_2) \triangleq \mathbf{E}\{h^*(t_1 - \alpha_1, \tau_1)h(t_2 - \alpha_2, \tau_2)\}. \quad (42)$$

Many wireless communications channels can be modeled to possess channel statistics that remain "stationary" over short time intervals (or over small spatial distances). To be precise, these channels are not necessarily stationary in a "strict-sense" nor in the "second-order." However, under translations over short time intervals, their second-order statistics are invariant, and can be approximated as being wide-sense stationary (WSS).⁸ For a slowly varying WSSUS channel, the correlation

⁸Definitions for different kinds of stationary can be found in [37].

$$R_y(t_1, t_2) = \begin{cases} \int_{-\infty}^{+\infty} P_h(0, \tau) \tilde{R}_s^*(t_1 - T_s - \tau) \tilde{R}_s(t_2 - T_s - \tau) d\tau, & |t_2 - t_1| < \frac{2}{B_s} \\ 0, & \text{otherwise} \end{cases} \quad (43)$$

function of the MFEP output is derived in [38] as (43) shown at the top of the page, where $P_h(0; \tau)$ is the PDP, also known as the multipath intensity profile, and

$$\tilde{R}_s(t - T_s - \tau) \triangleq \int_0^{+\infty} s(t - \alpha - \tau) f_M(\alpha) d\alpha. \quad (44)$$

In SS parlance, $\tilde{R}_s(\tau)$ is the periodic time autocorrelation function of the baseband spread signature sequence. For sequence designs as in [39], the function $\tilde{R}_s(\tau)$ possesses small sidelobes and has a narrow peak over the interval $|\tau| < 1/B_s$, where B_s denotes the spreading BW which is roughly equal to the chip rate R_c defined by $R_c = 1/T_c$. The symbol time T_s is equal to the chip duration times the processing gain of the SS system. In deriving (43), we have assumed that the sidelobes of $\tilde{R}_s(\tau)$ are zero.

The correlation function of $n_M(t)$ can be derived similarly as

$$\begin{aligned} R_n(t_1, t_2) &= \int_0^{+\infty} \int_0^{+\infty} \mathbb{E}\{n^*(t_1 - \alpha_1) n(t_2 - \alpha_2)\} \\ &\quad \times f_M^*(\alpha_1) f_M(\alpha_2) d\alpha_1 d\alpha_2 \\ &= 2N_0 \tilde{R}_s(t_2 - t_1). \end{aligned} \quad (45)$$

In deriving (45), we have used the property that $\mathbb{E}\{n^*(t_1 - \alpha_1) n(t_2 - \alpha_2)\} = 2N_0 \delta_D(t_2 - t_1 + \alpha_1 - \alpha_2)$, where $\delta_D(\cdot)$ is the Dirac delta function.

ACKNOWLEDGMENT

The authors wish to thank Z. A. Kostić, J. H. Winters, J. G. Proakis, L. J. Greenstein, G. J. Foschini, L. A. Shepp, N. C. Beaulieu, and P. F. Dahm for helpful discussions.

REFERENCES

- [1] R. L. Pickholtz, D. L. Schilling, and L. B. Milstein, "Theory of spread-spectrum communications—A tutorial," *IEEE Trans. Commun.*, vol. COM-30, pp. 855–884, May 1982.
- [2] R. L. Peterson, R. E. Ziemer, and D. E. Borth, *Introduction to Spread Spectrum Communications*, 1st ed. Englewood Cliffs, NJ: Prentice-Hall, 1995.
- [3] F. Adachi, M. Sawahashi, and H. Suda, "Wideband DS-CDMA for next-generation mobile communications systems," *IEEE Commun. Mag.*, vol. 36, pp. 56–69, Sept. 1998.
- [4] R. Price and P. E. Green, Jr., "A communication technique for multipath channels," *Proc. IRE*, vol. 46, pp. 555–570, March 1958.
- [5] G. Turin, "Introduction to spread-spectrum antimultipath techniques and their application to urban digital radio," *Proc. IEEE*, vol. 68, pp. 328–353, Mar. 1980.
- [6] J. S. Lehnert and M. B. Pursley, "Multipath diversity reception of spread spectrum multiple-access communications," *IEEE Trans. Commun.*, vol. COM-35, pp. 1189–1198, Nov. 1987.
- [7] J. G. Proakis, *Digital Communications*, 3rd ed. New York: McGraw-Hill, 1995.
- [8] M. Z. Win and R. A. Scholtz, "On the energy capture of ultra-wide bandwidth signals in dense multipath environments," *IEEE Commun. Lett.*, vol. 2, pp. 245–247, Sept. 1998.
- [9] F. Adachi, K. Ohno, A. Higashi, T. Dohi, and Y. Okumura, "Coherent multicode DS-CDMA mobile radio access," *IEICE Trans. Commun.*, vol. E79-B, pp. 1316–1324, Sept. 1996.
- [10] L. F. Chang, "Dispersive fading effects in CDMA radio systems," in *Proc. IEEE Int. Conf. Universal Personal Commun.*, Dallas, TX, Oct. 1992, pp. 185–189.
- [11] J. H. Holtzman and L. M. Jalloul, "Rayleigh fading effect reduction with wideband DS/CDMA signals," *IEEE Trans. Commun.*, vol. 42, pp. 1012–1016, Feb./Mar./Apr. 1994.
- [12] F. Amoroso and W. W. Jones, "Geometric model for DSPN satellite reception in the dense scatterer mobile environment," *IEEE Trans. Commun.*, vol. 41, pp. 450–453, Mar. 1993.
- [13] L. M. Jalloul and J. H. Holtzman, "Multipath fading effect on wide-band DS/CDMA signals: Analysis, simulation, and measurements," *IEEE Trans. Veh. Technol.*, vol. 43, pp. 801–807, Aug. 1994.
- [14] T. Eng and L. B. Milstein, "Coherent DS-CDMA performance in Nakagami multipath fading," *IEEE Trans. Commun.*, vol. 43, pp. 1134–1143, Feb./Mar./Apr. 1995.
- [15] L. M. Jalloul and J. H. Holtzman, "Performance analysis of DS/CDMA with noncoherent M -ary orthogonal modulation in multipath fading channels," *IEEE J. Select. Areas Commun.*, vol. 12, pp. 862–870, June 1994.
- [16] D. L. Noneaker and M. B. Pursley, "On the chip rate of CDMA systems with doubly selective fading reception," *IEEE J. Select. Areas Commun.*, vol. 12, pp. 853–861, June 1994.
- [17] D. Goeckel and W. Stark, "Performance of coded direct-sequence systems with rake reception in a multipath fading environment," *European Trans. Telecommun., Special Issue Spread Spectrum Techniques*, vol. 6, pp. 41–52, Jan.–Feb. 1995.
- [18] R. A. Scholtz and M. Z. Win, "Impulse radio," in *Wireless Communications*, S. G. Glisic and P. A. Leppänen, Eds. Norwell, MA: Kluwer Academic Publishers, 1997.
- [19] T. Eng, N. Kong, and L. B. Milstein, "Comparison of diversity combining techniques for Rayleigh-fading channels," *IEEE Trans. Commun.*, vol. 44, pp. 1117–1129, Sept. 1996.
- [20] H. Erben, S. Zeisberg, and H. Nuszowski, "BER performance of a hybrid SC/MRC 2DPSK RAKE receiver in realistic mobile channels," in *Proc. 44th Annu. Int. Veh. Technol. Conf.*, vol. 2, Stockholm, Sweden, June 1994, pp. 738–741.
- [21] N. Kong and L. B. Milstein, "Combined average SNR of a generalized diversity selection combining scheme," in *Proc. IEEE Int. Conf. Commun.*, vol. 3, Atlanta, GA, June 1998, pp. 1556–1560.
- [22] M. Z. Win and J. H. Winters, "Analysis of hybrid selection/maximal-ratio combining in Rayleigh fading," in *Proc. IEEE Int. Conf. Commun.*, vol. 1, Vancouver, Canada, June 1999, pp. 6–10.
- [23] Y. C. Yoon, R. Kohno, and H. Imai, "A spread-spectrum multiaccess system with cochannel interference cancellation for multipath fading channels," *IEEE J. Select. Areas Commun.*, vol. 11, pp. 1067–1075, Sept. 1993.
- [24] B. R. Vojčić and R. L. Pickholtz, "Performance of coded direct sequence spread spectrum in a fading dispersive channel with pulse jamming," *IEEE J. Select. Areas Commun.*, vol. 8, pp. 934–942, Sept. 1990.
- [25] G. L. Turin, "The effects of multipath and fading on the performance of direct-sequence CDMA systems," *IEEE J. Select. Areas Commun.*, vol. SAC-2, pp. 597–603, July 1993.
- [26] G. Turin, F. D. Clapp, T. L. Johnston, S. B. Fine, and D. Lavry, "A statistical model of urban multipath propagation," *IEEE Trans. Veh. Technol.*, vol. VT-21, pp. 1–9, Feb. 1972.
- [27] H. Hashemi, "Simulation of the urban radio propagation channel," *IEEE Trans. Veh. Technol.*, vol. VT-28, pp. 213–225, Aug. 1979.
- [28] D. C. Cox and R. P. Leck, "Distributions of multipath delay spread and average excess delay for 910-MHz urban mobile radio paths," *IEEE Trans. Antennas Propagat.*, vol. AP-23, pp. 206–213, Mar. 1975.
- [29] P. F. Driessen, "Prediction of multipath delay profiles in mountainous terrain," *IEEE J. Select. Areas Commun.*, vol. 18, pp. 336–346, Mar. 2000.
- [30] P. A. Bello, "Characterization of randomly time-variant linear channels," *IEEE Trans. Commun. Syst.*, vol. CS-11, pp. 360–393, Dec. 1963.

- [31] J. D. Parsons, *The Mobile Radio Propagation Channel*, 1st ed. New York: Wiley, 1992.
- [32] T. F. Wong, T. M. Lok, and J. S. Lehnert, "Asynchronous multiple-access interference suppression and chip waveform selection with aperiodic random sequences," *IEEE Trans. Commun.*, vol. 47, pp. 103–114, Jan. 1999.
- [33] J. W. Craig, "A new, simple and exact result for calculating the probability of error for two-dimensional signal constellations," in *Proc. Military Comm. Conf.*, Boston, MA, 1991, pp. 25.5.1–25.5.5.
- [34] C. Tellambura, A. J. Mueller, and V. K. Bhargava, "Analysis of M -ary phase-shift keying with diversity reception for land-mobile satellite channels," *IEEE Trans. Veh. Technol.*, vol. 46, pp. 910–922, Nov. 1997.
- [35] M.-S. Alouini and A. Goldsmith, "A unified approach for calculating error rates of linearly modulated signals over generalized fading channels," in *Proc. IEEE Int. Conf. Commun.*, vol. 1, Atlanta, GA, June 1998, pp. 459–463.
- [36] P. J. Bickel and K. Doksum, *Mathematical Statistics: Basic Ideas and Selected Topics*, 1st ed. Oakland, CA: Holden-Day, 1977.
- [37] W. A. Gardner, *Introduction to Random Processes with Applications to Signals and Systems*, 2nd ed. New York: McGraw-Hill, 1990.
- [38] M. Z. Win and Z. A. Kostić, "Impact of spreading bandwidth on Rake reception in dense multipath channels," in *Proc. 8th Comm. Theory Mini Conf.*, Vancouver, Canada, June 1999, pp. 78–82.
- [39] S. W. Golomb, *Shift Register Sequences*, rev. ed. Laguna Hills, CA: Aegean Park Press, 1982.



Moe Z. Win (S'85–M'87–SM'97) received the B.S. degree (*magna cum laude*) from Texas A&M University, College Station, and the M.S. degree from the University of Southern California (USC), Los Angeles, in 1987 and 1989, respectively, in electrical engineering. As a Presidential Fellow at USC, he received both an M.S. degree in applied mathematics and the Ph.D. degree in electrical engineering in 1998.

In 1987, he joined the Jet Propulsion Laboratory (JPL), California Institute of Technology, Pasadena.

From 1994 to 1997, he was a Research Assistant with the Communication Sciences Institute, where he played a key role in the successful creation of the Ultra-Wideband Radio Laboratory at USC. Since 1998, he has been with the Wireless Systems Research Department, AT&T Laboratories-Research, Red Bank, NJ, where he is a Principal Technical Staff Member. His main research interests are the application of communication, detection, and estimation theories to a variety of communications problems including time-varying channels, diversity, equalization, synchronization, signal design, ultrawide-bandwidth communication, and optical communications.

Dr. Win is a member of Eta Kappa Nu, Tau Beta Pi, Pi Mu Epsilon, Phi Theta Kappa, and Phi Kappa Phi. He was a University Undergraduate Fellow at Texas A&M University, where he received, among others awards, the Academic Excellence Award. At USC, he received several awards including the Outstanding Research Paper Award and the Phi Kappa Phi Student Recognition Award. He was the recipient of the IEEE Communications Society Best Student Paper Award at the Fourth Annual IEEE NetWorld + Interop'97 Conference. He has been involved in chairing and organizing sessions in a number of IEEE conferences. He served as a member of the Technical Program Committee for the IEEE Communication Theory Symposium during Globecom'99, the 1999 IEEE Wireless Communications and Networking Conference, and the 1999 IEEE 49th Annual International Vehicular Technology Conference; and as a member of the International Advisory Committee for the 1999 IEEE 50th International Vehicular Technology Conference. He currently serves as the Tutorial Chair for the 2001 IEEE International Vehicular Technology Conference and the Technical Program Chair for the IEEE Communication Theory Symposium during Globecom 2000. He is the current Editor for *Equalization and Diversity* for the IEEE TRANSACTIONS ON COMMUNICATIONS.



George Chrisikos (S'91–M'98) received the Ph.D. in electrical engineering from the University of Southern California (USC), Los Angeles under the USC Dean's Doctoral Merit Fellowship. He received the B.S. and M.S. degrees in electrical engineering from the University of New Mexico (UNM), Albuquerque, where he was a Presidential Scholar. He graduated Summa Cum Laude with Distinction and was the Valedictorian of his class.

He has been working in the research, design, development, and implementation of communication systems and algorithms for wireless, satellite, and wireline applications. He held positions at the Center for High Technology Materials, at TRW, and the Sandia National Laboratories. He was with The Aerospace Corporation in Los Angeles as a Senior Member of the Technical Staff where he was awarded the Aerospace Corporate Achievement Award. He is now with Dot Wireless Inc., a start-up company in San Diego where he is responsible for communication systems engineering and design based on the 2nd and 3rd Generation CDMA standard for cellular and PCS communications.

Dr. Chrisikos is a member of Tau Beta Pi, Eta Kappa Nu, Phi Kappa Phi, Kappa Mu Epsilon and has been elected to *Who's Who in Science and Engineering* and *Who's Who in the World*. He has been involved in organizing and chairing sessions at IEEE conferences. He is on the Technical Program Committee of the IEEE Wireless Communications and Networking Conference (WCNC'99), the IEEE Global Communications Conference (Globecom 2000), and is a representative for the Communication Theory Technical Committee for Globecom 2000.



Nelson R. Sollenberger (S'78–M'81–SM'90–F'96) heads the Wireless Systems Research Department at AT&T. His department performs research on next generation wireless systems concepts and technologies including high speed transmission methods, smart antennas and adaptive signal processing, system architectures and radio link techniques to support wireless multimedia and advanced voice services.

He received his Bachelor's degree from Messiah College (1979) and his Master's degree from Cornell University (1981), both in electrical engineering. From 1979 through 1986, he was a member of the cellular radio development organization at Bell Laboratories. At Bell Laboratories, he investigated spectrally efficient analog and digital technologies for second-generation cellular radio systems. In 1987, he joined the Radio Research Department at Bellcore, and was the Head of that department from 1993 to 1995. At Bellcore, he investigated concepts for PACS, the Personal Access Communications System. In 1995, he joined AT&T.